DOI:
10.1002/mrm.25362

Document Version
Publisher's PDF, also known as Version of record

Kinetic Analysis of Hyperpolarized Data with Minimum a Priori Knowledge: Hybrid Maximum Entropy and Nonlinear Least Squares Method (MEM/NLS)

Erika Mariotti,[1]* Mattia Veronese,[2] Joel T. Dunn,[1] Richard Southworth,[1] and Thomas R. Eykyn[1]

Purpose: To assess the feasibility of using a hybrid Maximum-Entropy/Nonlinear Least Squares (MEM/NLS) method for analyzing the kinetics of hyperpolarized dynamic data with minimum a priori knowledge.

Theory and Methods: A continuous distribution of rates obtained through the Laplace inversion of the data is used as a constraint on the NLS fitting to derive a discrete spectrum of rates. Performance of the MEM/NLS algorithm was assessed through Monte Carlo simulations and validated by fitting the longitudinal relaxation time curves of hyperpolarized [1-^{13}C] pyruvate acquired at 9.4 Tesla and at three different flip angles. The method was further used to assess the kinetics of hyperpolarized pyruvate-lactate exchange acquired in vitro in whole blood and to re-analyze the previously published in vitro reaction of hyperpolarized ^{15}N choline with choline kinase.

Results: The MEM/NLS method was found to be adequate for the kinetic characterization of hyperpolarized in vitro time-series. Additional insights were obtained from experimental data in blood as well as from previously published ^{15}N choline experimental data.

Conclusion: The proposed method informs on the compartmental model that best approximate the biological system observed using hyperpolarized ^{13}C MR especially when the metabolic pathway assessed is complex or a new hyperpolarized probe is used. **Magn Reson Med 73:2332–2342, 2015.**

Key words: kinetic modeling; hyperpolarization; MEM/NLS method

INTRODUCTION

Hyperpolarized metabolic imaging has enabled significant enhancements of the magnetic resonance (MR) signals of ^{13}C in a range of small molecules allowing the distinction and imaging of an injected molecule from its downstream metabolites. It has received much interest for the real-time study of kinetics of a range of metabolic processes in cancer (1), the heart (2), the liver (3), and in the brain (4). Metabolic conversion of hyperpolarized molecules can be studied in vitro in whole cells, ex vivo in perfused organs as well as in vivo. The acquisition of a time-series of hyperpolarized MR spectra leads to multi-exponential temporal dynamics that contain information on the underlying metabolic reactions, membrane transport rates, enzyme activities, availability of enzyme cofactors etc.

Dynamic curves can be fitted using different analysis methods to quantify the rates of the kinetic processes described in the data. A common approach to fit hyperpolarized data uses mathematical models characterized by several compartments that interconvert at characteristic rates. This method has been used to quantify the rate of conversion of hyperpolarized pyruvate to lactate in vitro in EL-4 mouse lymphoma cells (1) and in T47D human breast cells (5), as well as to characterize pyruvate metabolism in pig hearts in vivo (6). Compartmental modeling requires a knowledge of the chemical products of the reaction but also a priori assumption of the nature of the enzymatic reactions involved in the process. If the first point does not represent an issue because the number of metabolites can be identified by the number of peaks in the spectrum, the second point is more challenging particularly if the metabolic pathways are complex. A similar problem is encountered for the kinetic analysis of time-activity curves acquired using Positron Emission Tomography (PET). In this case it is often difficult to select a compartmental model among those possible that best approximates the interaction of the PET tracer with the region of interest (ROI). Spectral-based algorithms which require minimum a priori assumptions have been proposed as an alternative approach to compartmental modeling for the kinetic analysis of PET dynamic data (7,8). In this work we explore the possibility of using a hybrid maximum entropy/nonlinear least squares method (MEM/NLS) for the kinetic characterization of dynamic hyperpolarized ^{13}C data. This approach was originally proposed for the analysis of protein folding by *Steinbach and colleagues* and similarly to spectral-based algorithms allows the derivation of a spectrum of kinetic rates that characterize the

[1]Division of Imaging Sciences and Biomedical Engineering, St. Thomas' Hospital, King's College London, London, United Kingdom.

[2]Institute of Psychiatry, King's College London, London, United Kingdom.

*Correspondence to: Erika Mariotti, Ph.D., King's College London, Division of Imaging Sciences and Biomedical Engineering, 4th Floor, Lambeth Wing, St. Thomas' Hospital, Westminster Bridge Road, London SE1 7EH.
E-mail: erika.mariotti@kcl.ac.uk

The copyright line for this article was changed on 17 September 2014 after original online publication.

Received 27 March 2014; revised 11 June 2014; accepted 23 June 2014

DOI 10.1002/mrm.25362
Published online 15 July 2014 in Wiley Online Library (wileyonlinelibrary.com).

biological phenomena described in the experimental data with minimum a priori assumptions (9).

Spectral-based algorithms, and similarly the MEM/NLS algorithm, can be applied only to single input systems, described by a set of first order linear differential equations (no input delay or input dispersion terms included). These assumptions, do not represent a restriction for their applicability because they are commonly satisfied by the systems assessed using hyperpolarized ^{13}C MR (10).

The performance of the MEM/NLS algorithm for the kinetic analysis of hyperpolarized in vitro ^{13}C time-series was studied using Monte Carlo simulations over a range of known kinetics. The proposed method was validated by fitting the characteristic relaxation curves of hyperpolarized [1-^{13}C] pyruvate acquired at 9.4T using three different flip angles. Additionally, we used the MEM/NLS algorithm to assess the kinetics of time-series of hyperpolarized ^{13}C pyruvate-lactate exchange acquired in vitro in whole blood cells as well as to re-analyze the previously published in vitro reaction of hyperpolarized ^{15}N choline with choline kinase (11).

THEORY

The conversion of a hyperpolarized molecule to its downstream metabolites in vitro can be modeled as a multi-compartmental system described by the Bloch-McConnell equations that include both the effect of chemical reaction and relaxation of the hyperpolarized MR signal (Eq. [1]) (1).

$$\frac{d\mathbf{M}(t)}{dt} = (\mathbf{K} - \mathbf{R})\mathbf{M}(t) \qquad [1]$$

$\mathbf{M}(t)$ is a time dependent vector of length N of the longitudinal magnetizations M_z, $\mathbf{K}$ is a N×N matrix whose elements k are the characteristic rates of the compartmental model chosen and $\mathbf{R}$ is the relaxation matrix containing the longitudinal relaxation rates $r_1 = 1/T_1$ or accounting for the influence of flip angle (θ) can be modified with effective relaxation rates $r_1 = 1/T_1 - \ln(\cos\theta)/TR$ for a given repetition time TR. The dimension of the system N depends on the number of metabolites detected after the injection of the hyperpolarized probe into the system of interest. Each element of the vector $\mathbf{M}(t)$ gives the evolution in time of one compartment.

The solution of the general system of differential equations presented in Eq. [1] to an impulse input can be formulated for a given metabolite as a function M(t) given by a discrete set of n exponentials:

$$M(t) = \sum_{i=1}^{n} A_i \exp(-\lambda_i t) \qquad [2]$$

where A_i are the characteristic amplitudes of the rates λ_i. The rates λ_i correspond to the eigenvalues of the matrix (**K**-**R**) in Eq. [1] and are, therefore, combinations of the rates of exchange between compartments and the relaxation rates. The value of n depends on the type of interaction between the compartments (i.e., uni- or bi-directional). For instance, the solution of the differential equation in Eq. [1] for a two compartment bi-directional in vitro system shown in Figure 1 is characterized by $n = 2$ (bi-exponential kinetics) for both compartment A and B.

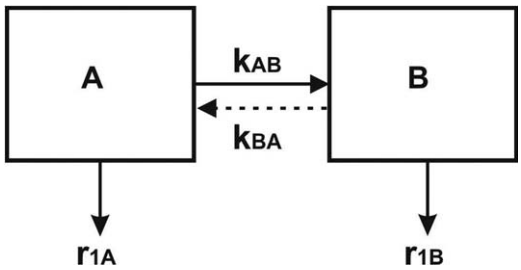

FIG. 1. Two-compartment kinetic model. The forward conversion of A to B is represented with a continuous arrow (k_{AB}), whereas the back reaction converting B to A is plotted with a dotted arrow (k_{BA}).

For a two-compartment, uni-directional system the dynamics of compartment A is characterized by $n = 1$ (mono-exponential) and compartment B by $n = 2$ (bi-exponential).

In compartmental modeling the problem of finding the optimal value for A_i, λ_i, and n is often formulated as an optimization problem and Eq. [2] is fit to the experimental data using a nonlinear least square (NLS) algorithm.

Instead of imposing a (discrete) compartmental model, experimental data can alternatively be fitted with a continuous distribution of exponential rates $g(\lambda)$ as follows (12):

$$M(t) = \int_0^\infty g(\lambda)\exp(-\lambda t)d\rho \qquad [3]$$

The distribution that best describes the data is obtained by applying the inverse Laplace transform to M(t) without any assumption on the structure of the data. The Laplace inversion of experimental data characterized by random noise is an ill-posed problem (i.e., an infinite number of solutions is available) and a regularization strategy is required to find the optimal distributions $g(\lambda)$. The maximum entropy method (MEM) finds the unique optimum distributions $g(\lambda)$ by maximizing the following cost function (13):

$$Q = S - \alpha\chi^2 \qquad [4]$$

S is the entropy term and χ^2 is the normalized mean square error. α is the Lagrange multiplier varied during the optimization processes to maintain χ^2 small while maximizing S. This approach gives a unique solution independent of initial guess of the model parameters. MEM, however, biases the results leading to nonrandom residuals (9).

MEM/NLS combines the advantages of NLS with those of MEM. Using this approach, the distribution of rates that best describe the experimental data is derived without any a priori assumption of the number of the kinetic components described in the time-series; it is unique and not biased. The algorithm is based on an iterative process that exploits a continuous distribution derived from the inversion of the experimental data through MEM to insert one exponential at a time into the NLS fit. Every time the MEM algorithm converges the number of peaks n in the continuous distribution is characterized and the NLS fit is performed with one exponential more than those used at the previous iteration. If the number of peaks in the continuous distribution is increased by

more than one from the previous iteration, only the $n+1$ peaks characterized by the largest area are considered for the NLS fit in an iterative process until all the peaks that appear in the continuous distribution are accounted for in the discrete fit. The chosen optimal MEM distribution is found when χ^2 has decreased by less than 1% with respect to the previous optimization. The optimal NLS fit is that characterized by several exponentials, n, for which χ^2 has decreased by less than 1% from the discrete distribution characterized by n-1 kinetic rates (9). The final solution of the hybrid MEM/NLS is a discrete distribution of rates whose number n is that which best describes the nature of the data.

As for spectral-based algorithms in PET, it is possible, under certain hypotheses, to associate a compartmental model to the MEM/NLS solution and derive the characteristic rates of metabolic conversion (see Appendix for details). An advantage of this method is that no a priori assumption on the structure of the metabolic pathway has to be specified. Thus it represents a valid alternative to compartmental modeling when a certain degree of uncertainty on the metabolic pathway of the system is present.

METHODS

Monte Carlo Simulations

The dynamics of in vitro uni- and bi-directional systems were simulated using the Bloch-McConnell equations (Eq. [1]) written for a two-compartment, bi-directional reaction system, in which a given chemical compound is converted to a single product (Fig. 1) (Eqs. [5–8]).

$$\frac{dM_A(t)}{dt} = -(k_{AB} + r_{1A})M_A(t) + k_{BA}M_B(t) \quad [5]$$

$$\frac{dM_B(t)}{dt} = k_{AB}M_A(t) - (k_{BA} + r_{1B})M_B(t) \quad [6]$$

$$M_A(0) = M_0 \quad [7]$$

$$M_B(0) = 0 \quad [8]$$

k_{AB} and k_{BA} are the two apparent rates of the enzymatic conversion. $r_{1A} = \frac{1}{T_{1A}} - \frac{1}{TR}\ln(\cos\theta)$ and $r_{1B} = \frac{1}{T_{1B}} - \frac{1}{TR}\ln(\cos\theta)$ representing the effective relaxation rates of the hyperpolarized signal of A and B, respectively, that take into account the loss of signal due to T_1 and the application of the RF excitation pulse characterized by a flip angle θ and time repetition TR (14). M_0 represents the intensity of the hyperpolarized signal of compartment A at $t=0$. The values used in the simulation for k_{AB} and k_{BA} are reported in Table 1. r_{1A} and r_{1B} were randomly generated within a chosen interval ($0.022\ s^{-1} < r_{1A} < 0.04\ s^{-1}$ and $0.03\ s^{-1} < r_{1B} < 0.05\ s^{-1}$) for both uni- and bi-directional systems. All rate values were chosen within a physiological range characteristic of the in vitro conversion of pyruvate to lactate catalyzed by lactate dehydrogenase (LDH) and in agreement with previous studies (5,14,15). To assess the influence of random noise in the data, each dataset was simulated for a low and a high signal-to-noise ratio (SNR) (SNR = 20 and SNR = 90) in the range of those found in our experimental data. Usually the lowest SNR detected in vitro is associated with the hyperpolarized time-series for the product of the metabolic conversion, in this case represented by compartment B. The SNR was calculated as the ratio between the maximum value of the time-signal intensity curve of compartment B and the standard deviation of the noise of the same curve at thermal equilibrium (SNR_B) (16). Datasets were simulated with a time resolution $\Delta t = 2$ s and repeated 100 times at each set of parameters. All simulated datasets were fitted with the MEM/NLS algorithm and the ability of the method to derive the correct number of known kinetic components in the simulated data was assessed.

Table 1
Values Used for the Apparent Constant Rates in the Monte Carlo Simulations

	Bi-directional		Uni-directional	
	k_{AB}	k_{BA}	k_{AB}	k_{BA}
system 1	0.02	0.002	0.002	0
system 2	0.04	0.004	0.004	0
system 3	0.06	0.006	0.006	0
system 4	0.08	0.008	0.008	0

k_{AB} and k_{BA} indicate the apparent rates of enzymatic conversion. Units are in s^{-1}.

The values of M_0, r_{1A}, r_{1B}, k_{AB}, and k_{BA} were derived by associating a compatible compartmental model to the MEM/NLS solution and solving the system of algebraic equations shown in the Appendix (Eqs. [A3–A6] and Eqs. [A10–A14] for bi- and uni-directional systems, respectively). These values were compared with the simulated reference values as well as to the estimates derived using conventional compartmental modeling. The percent bias (%BIAS) for the kinetic rates k_{AB} and k_{BA} was calculated as a performance index:

$$\%BIAS_p = 100 * \sum_{j=1}^{k} \frac{(p_j - p_{TRUE})}{p_{TRUE}} \quad [9]$$

where p_j and p_{TRUE} are the estimated and true value of the indices p.

Monte Carlo simulations were performed using a custom-made Matlab (MathWorks®) code, whereas the fitting was performed with MeMExp software (9) available online http://cmm.cit.nih.gov/memexp.

Experimental

Samples containing [1-^{13}C] pyruvic acid, 15 mM trityl radical and 1 mM Gadolinium (Dotarem) were hyperpolarized in a HyperSense® (Oxford Instruments) DNP at 3.35T and 1.4K for ~ 1 hr. Dissolution was performed using 4 mL of 40 mM TRIS buffer, 1 mM EDTA and neutralized to pH 7 with NaOH to yield a final solution of 50 mM hyperpolarized pyruvate. Experiments carried out on whole blood cells also included 50 mM unpolarized sodium lactate in the dissolution buffer. Polarizations were typically of the order P = 20%.

Hyperpolarized [1-^{13}C] Pyruvate in Solution

Experiments were performed on a Bruker 9.4T Avance III spectrometer using a BBO broad-band observe probe at

298K. The hyperpolarized sample was contained in a 5-mm tube with susceptibility matched plugs to restrict the sample volume to the active region of the coil.

Hyperpolarized spectra were acquired from three identical hyperpolarized [1-^{13}C] pyruvate samples with a single acquisition using three different small flip angles: $\theta = 1^\circ$, $\theta = 5^\circ$, $\theta = 10^\circ$. Hyperpolarized time-series were acquired with a temporal resolution $\Delta t = 2$ s. The effective relaxation time constants of [1-^{13}C] pyruvate which include the influence of T_1 and flip angle (θ) was derived by fitting the dynamic time-series of the hyperpolarized signal decay with both a mono-exponential function and the MEM/NLS algorithm and the results were compared.

Hyperpolarized [1-^{13}C] Pyruvate in Whole Blood

All procedures involving animals were carried out in accordance with the Home Office Guidance on the Operation of Animals (Scientific Procedures) Act 1986, HMSO (London). Blood samples were collected in heparinized MR tubes from male Wistar rats (250–300 g, $n = 4$) under terminal anesthesia at the same time as the excision of the heart for a separate experiment (17). A total of 100 μL of the hyperpolarized [1-^{13}C] pyruvate containing unlabelled sodium lactate were vigorously mixed with 500 μL of whole blood in a 5-mm MR tube before being inserted immediately into the bore of a Bruker 9.4T Avance III spectrometer. We assume mixing of the hyperpolarized solution and the blood cells to be instantaneous. Time-series of hyperpolarized ^{13}C MR spectra ($\Delta t = 2$ s) were acquired on a Bruker 9.4T at 310K and a small flip angle excitation ($\theta = 10^\circ$). ^{13}C hyperpolarized MR spectra were integrated and the resulting time-series fitted with the hybrid MEM/NLS method (MeMExp software). The kinetic rates obtained using this approach were compared with those derived by fitting the data with a traditional compartmental model.

Hyperpolarized ^{15}N Choline

Hyperpolarized ^{15}N data analyzed in this work were previously published (11). ^{15}N labeled choline chloride mixed with 15 mM of trityl free radical (OX63) and DMSO/H_2O was hyperpolarized at low temperature (1.4 K) for 2 h. After dissolution, a 20 mM choline hyperpolarized solution was collected in an MR tube containing purified human choline kinase and 10 mM ATP as cofactor for the enzyme reaction. A series of ^{15}N MR spectra ($\Delta t = 3.67$ s) of hyperpolarized choline and its metabolic product phosphocholine was detected on a 9.4T MR spectrometer. Previously, the resulting time-series were fitted with a two-compartment, uni-directional model (Fig. 1 with $k_{BA} = 0$). We re-analyzed these experimental data with the hybrid MEM/NLS algorithm and compared the results obtained from this method with those previously published (11).

RESULTS

The results from Monte Carlo simulations showed that the hybrid MEM/NLS algorithm is able to discern between bi- and uni-directional in vitro systems by estimating the number of exponentials that describe the data. In Figure 2 a representative result from the fitting of simulated data using the MEM/NLS method is shown for both bi- and uni-directional systems. The hybrid algorithm derives two rates for compartment B from the time-series of both systems simulated (black lines in Figures 2E and F), while two and one exponentials are identified from the dynamic curve of compartment A of a bi- and uni-directional system, respectively (blue lines in Figures 2E and F). This is in agreement with the solution of the Bloch-McConnell equations written for uni- and bi-directional systems.

The percentage error in estimating the number of components using the MEM/NLS algorithm is presented in Table 2 for both bi- and uni-directional systems. The ability of the hybrid method in deriving the correct number of rates from the time-series of compartment A was similar for the range of noise values simulated as well as for the simulated value of k_{AB} and $k_{BA.}$ The percentage correctness (CE) was $> 95\%$, with the exception of the bi-directional system simulated with the smallest k_{AB} and the highest noise ($CE = 64\%$). The ability of the algorithm to derive the correct number of exponentials from compartment B decreased with increasing values of k_{AB} for both simulated systems and was similar for the two SNR_B simulated.

Using the MEM/NLS algorithm it is possible to derive the values of the apparent kinetic rates k_{AB} and k_{BA} by associating a compatible compartmental model to the MEM/NLS solution and solving the systems of linear algebraic equations shown in the Appendix (Eqs. [A3–A6] and Eqs. [A10–A14] for bi and uni-directional systems, respectively). The values estimated for k_{AB} and k_{BA} using the MEM/NLS algorithm and those obtained by fitting the data with a corresponding compartmental model are plotted against the values used as input to the Monte Carlo simulations in Figure 3. For both types of systems the values of k_{AB} estimated using the hybrid algorithm are in excellent agreement with those derived through compartmental modeling and the real values (Figs. 3A and C) at the SNR_B and k_{AB} values considered. MEM/NLS algorithm is less accurate than traditional compartmental modeling in the estimation of small values of k_{BA}, nevertheless the values of k_{BA} reported using the hybrid method are in a linear relationship with the real input values (Fig. 3B).

For bi-directional systems the maximum value of $\%Bias_{kAB}$ and $\%Bias_{kBA}$ (mean $\pm$ SD) using the MEM/NLS algorithm was reported at $SNR_B = 20$ equal to $1\% \pm 6\%$ for $k_{AB} = 0.06$ s^{-1} and $-18\% \pm 57\%$ for $k_{BA} = 0.002$ s^{-1}, respectively. The minimum value of $\%Bias_{kAB}$ and $\%Bias_{kBA}$ was reported at $SNR_B = 90$ equal to $-0.3\% \pm 2\%$ for $k_{AB} = 0.06$ s^{-1} and to $22\% \pm 20\%$ for $k_{BA} = 0.008$ s^{-1}. For unidirectional systems, the maximum %Bias value reported for k_{AB} was $7\% \pm 18\%$ at $SNR_B = 20$ and $k_{AB} = 0.002$ s^{-1}, whereas the minimum value was $4\% \pm 3\%$ at $k_{AB} = 0.006$ s^{-1} and $SNR_B = 90$.

The MEM/NLS algorithm was used to fit the mono-exponential relaxation decays of hyperpolarized [1-^{13}C] pyruvate acquired in solution at 9.4T using three different flip angles $\theta = 1^\circ$, $\theta = 5^\circ$, $\theta = 10^\circ$ (Fig. 4A). The hybrid method correctly derived a single rate to describe the

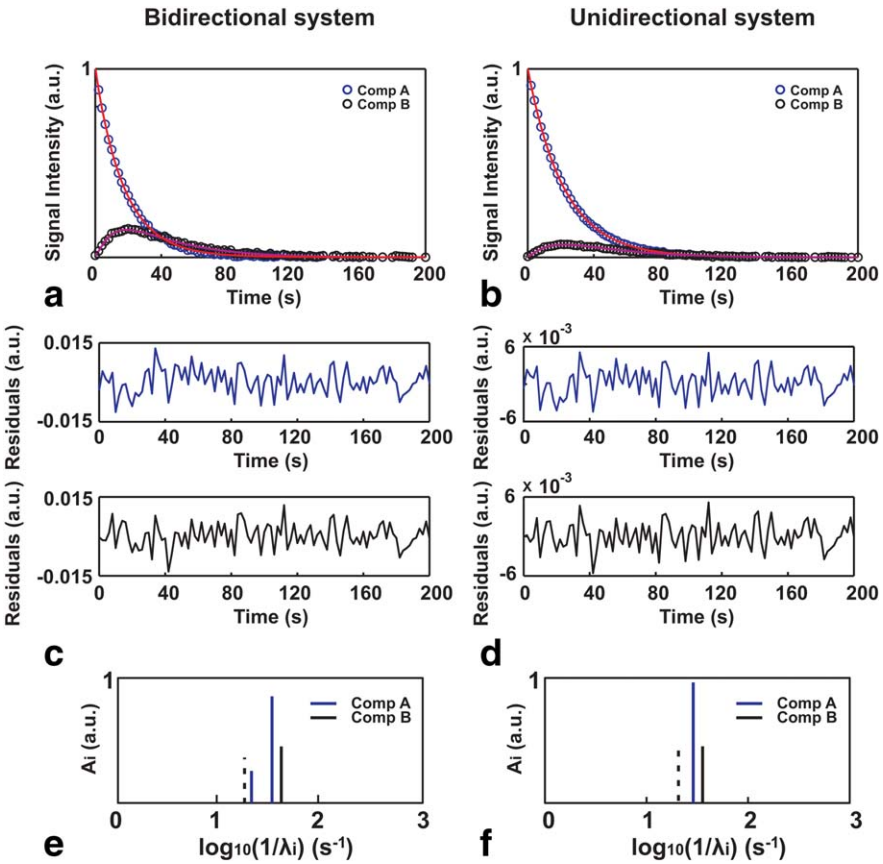

FIG. 2. Representative results from the hybrid MEM/NLS fit for bi-directional reaction kinetics, left panel, and uni-directional reaction systems, right panel. **a,b:** Show simulated datasets (colored dots) and overlaid fits (colored lines) plotted for compartments A (blue) and B (black). The residuals from the fits are plotted in blue and black for compartment A and B, respectively, in (**c**) and (**d**). **e,f:** show the kinetic rates resulted from the MEM/NLS analysis of the datasets shown in (a) and (b), respectively. Solid and dashed lines indicate rates with positive and negative amplitudes, respectively.

pyruvate decay curves corresponding to the relaxation rate of hyperpolarized [1-^{13}C] pyruvate which includes the effect of relaxation $r_{1p} = 1/T_{1p}$ and loss of polarization due to the flip angle (Fig. 4B). In Figure 4C the values of T_{1p} derived using MEM/NLS are plotted against those obtained fitting the experimental data with a mono-exponential function. The effective relaxation times reported using MEM/NLS were $T_{1p} = 54.5$ s, 51.1 s, and 41.6 s for a nominal flip angle equal to 1°, 5°, and 10°, respectively. For very low flip angles the decay of the signal is determined only by T_1 (e.g., $\cos^n(1°) \sim 1$ for $n < 100$ pulses). We can therefore calculate the true flip

Table 2
Performance of MEM/NLS algorithm in identifying the number of kinetic components from simulated datasets

BI-DIRECTIONAL SYSTEMS												
	Compartment A						Compartment B					
	SNR_B=20			SNR_B=90			SNR_B=20			SNR_B=90		
Simulated scenario	UE	OE	CE	UE	OE	CE	UE	OE	CE	UE	OE	CE
$k_{AB} = 0.02/k_{BA}$=0.002	36%	--	64%	--	2%	98%	2%	4%	94%	--	5%	95%
$k_{AB} = 0.04/k_{BA}$=0.004	4%	--	96%	5%	--	95%	4%	8%	88%	1%	13%	86%
$k_{AB} = 0.06/k_{BA}$=0.006	5%	--	95%	5%	--	95%	1%	22%	77%	1%	23%	76%
$k_{AB} = 0.08/k_{BA}$=0.008	2%	--	98%	1%	--	99%	11%	19%	70%	9%	21%	70%

UNI-DIRECTIONAL SYSTEMS												
	Compartment A						Compartment B					
	SNR_B=20			SNR_B=90			SNR_B=20			SNR_B=90		
Simulated scenario	UE	OE	CE	UE	OE	CE	UE	OE	CE	UE	OE	CE
$k_{AB} = 0.002$	--	--	100%	--	--	100%	1%	5%	94%	--	5%	95%
$k_{AB} = 0.004$	--	2%	98%	--	--	100%	2%	4%	94%	--	2%	98%
$k_{AB} = 0.006$	--	--	100%	--	--	100%	3%	4%	93%	--	2%	97%
$k_{AB} = 0.008$	--	--	100%	--	--	100%	5%	6%	89%	--	3%	97%

k_{AB} and k_{BA} indicate the apparent rates of enzymatic conversion. Units are in s^{-1}. UE = Underestimated number of components; OE = overestimated number of components; CE = correctly estimated.

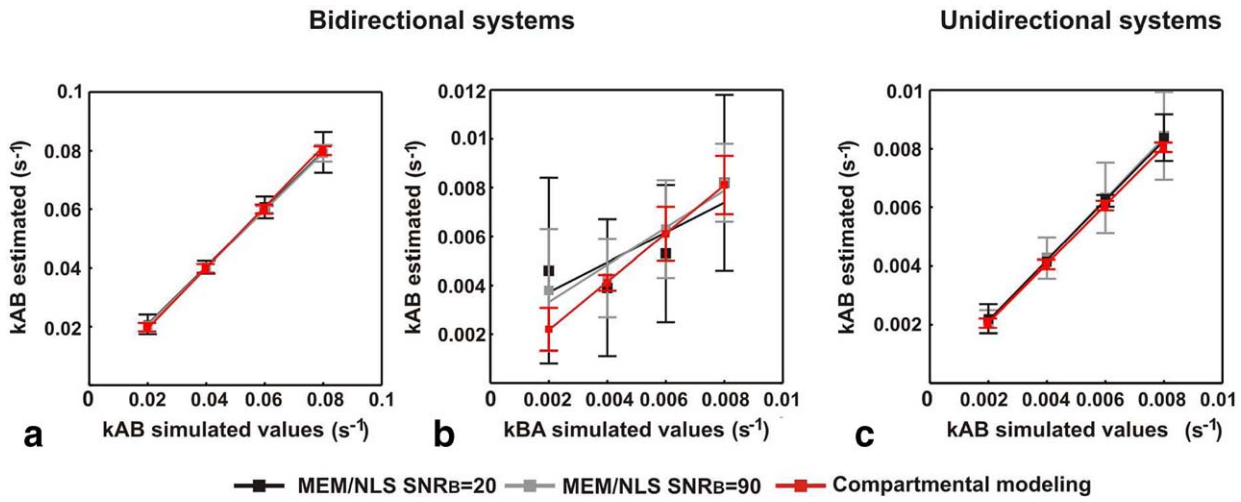

FIG. 3. **a,b:** Show the values of k_{AB} and k_{BA}, respectively, derived using the MEM/NLS algorithm for bi-directional systems plotted in black ($SNR_B = 20$) and grey ($SNR_B = 90$) against the real values used as input to the Monte Carlo simulations. The values estimated for the same rates using a conventional two-compartment, bi-directional kinetic model are plotted in the same figure in red. **c:** Shows the relationship between the values of k_{AB} estimated through the hybrid method in black ($SNR_B = 20$) and grey ($SNR_B = 90$) and the real values for uni-directional systems. The values estimated through a two-compartment, uni-directional kinetic model are plotted against the input values in red.

angles using the relation $T_{eff}^{-1} = T_1^{-1} - TR^{-1}\ln(\cos\theta)$ and a true $T_1 \sim 54.5$s to give actual flip angles of 4° and 8.6° which are less the nominal flip angles.

A representative hyperpolarized ^{13}C MR spectrum of pyruvate (~170 ppm) and its metabolite lactate (~183.5 ppm) in whole blood cells is shown in Figure 5A. The peak ~179 ppm corresponds to pyruvate hydrate, a nonmetabolically active compound formed when pyruvate reacts with water. The hyperpolarized time-series of pyruvate (blue) and lactate (black) with overlaid MEM/NLS fits (red) are plotted as a function of time in Figure 5B. Fitting residuals are presented in Figure 5C. Figure 5D shows the results of the MEM/NLS fits to the hyperpolarized ^{13}C data. One discrete rate was derived through the hybrid algorithm from the pyruvate curve (black line), whereas two rates were obtained from the lactate time-series (blue lines). This solution is compatible with a two-compartment, uni-directional compartmental model and, therefore, Eqs. [A10–A14] presented in the Appendix were used to derive the rate of enzymatic conversion of pyruvate (compartment A) to lactate (compartment B) k_{AB} as well as the relaxation rates r_{1A} and r_{1B}. The values estimated for

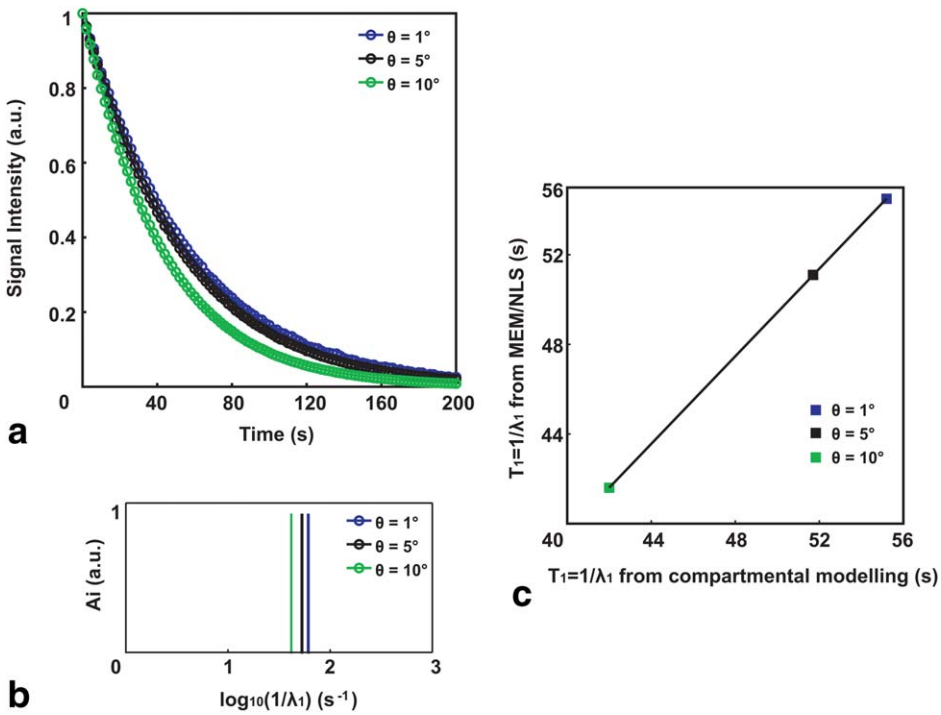

FIG. 4. **a:** Relaxation curves of [1-^{13}C] pyruvate at 9.4T acquired using $\theta = 1°$ (blue), $\theta = 5°$ (black) and $\theta = 10°$ (green) are plotted as a function of time with overlaid their MEM/NLS fit. **b:** Result from the MEM/NLS analysis of the datasets shown in (A). **c:** Relaxation time constants T_1 of [1-^{13}C] pyruvate derived using the MEM/NLS method are plotted against those obtained from a mono-exponential fit.

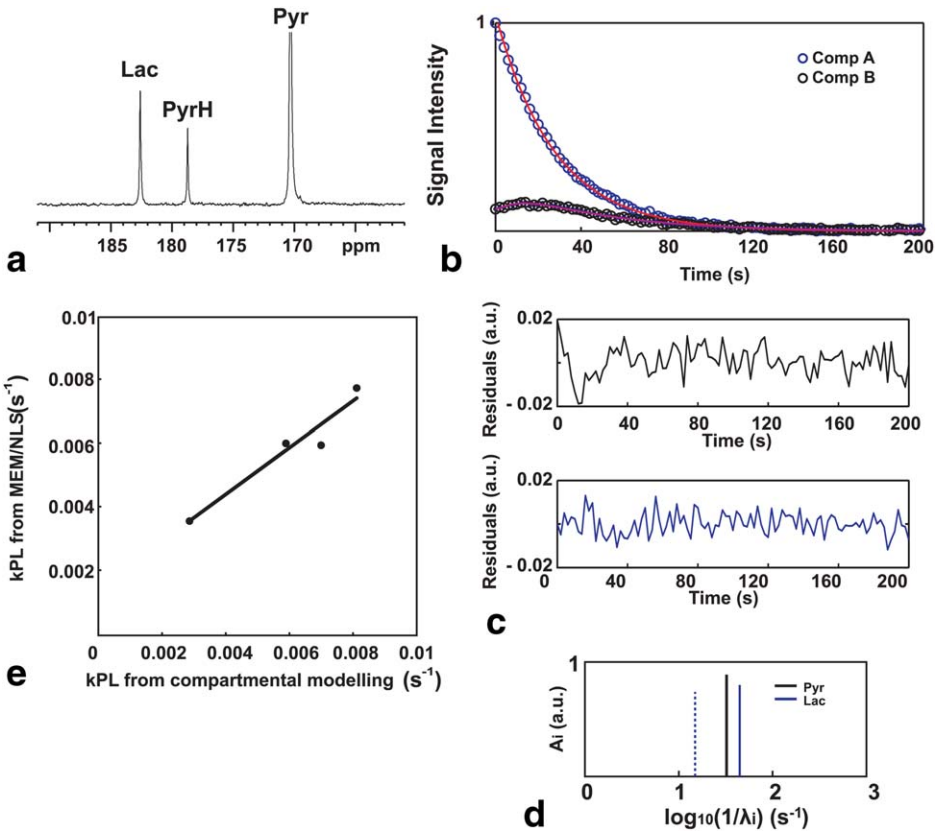

FIG. 5. **a:** Hyperpolarized ^{13}C spectrum of pyruvate and its metabolites lactate and pyruvate hydrate in whole blood cells. **b:** Shows representative fits to the data using the hybrid MEM/NLS method of pyruvate dynamics (blue) and lactate dynamics (black) in whole blood cells. **c:** Residuals to the fits are shown. **d:** Representative kinetic rates derived through the MEM/NLS analysis. Solid and dashed lines correspond to rates with positive and negative amplitude, respectively. **e:** The values of k_{AB} representing the rate of conversion of pyruvate to lactate derived using the MEM/NLS approach are plotted against those obtained fitting the experimental data with a two compartments, uni-directional kinetic model.

k_{AB} ($k_{AB} = 0.0058\ s^{-1} \pm 0.0020\ s^{-1}$, $n = 4$) are plotted against those derived using a two-compartment, uni-directional kinetic model ($k_{AB} = 0.0059\ s^{-1} \pm 0.0022\ s^{-1}$, $n = 4$) in Figure 5E. The values reported for k_{AB} derived using a two-compartment bi-directional kinetic model were found to be almost identical to those estimated with a uni-directional ($k_{AB} = 0.0058\ s^{-1} \pm 0.0024\ s^{-1}$). The algorithm failed in estimating the values of k_{BA} always returning the value of the lowest boundary condition set. The values reported using MEM/NLS for r_{1A} and r_{1B} were equal to $0.02\ s^{-1} \pm 0.002\ s^{-1}$ and $0.05\ s^{-1} \pm 0.01\ s^{-1}$, respectively. Fitting the experimental data with a two-compartment, uni-directional kinetic model the values obtained for r_{1A} and r_{1B} were $0.03\ s^{-1} \pm 0.004\ s^{-1}$ and $0.04\ s^{-1} \pm 0.005\ s^{-1}$, respectively. The values obtained for the rates of decay of the hyperpolarized signal of compartments A and B using a two-compartment, bi-directional model were $r_{1A} = 0.028\ s^{-1} \pm 0.005\ s^{-1}$, $r_{1B} = 0.034\ s^{-1} \pm 0.011\ s^{-1}$. The SNR_B reported for these datasets was 35 ± 10 (a.u.) in agreement with the values used in the Monte Carlo simulations.

In vitro hyperpolarized ^{15}N experimental data are presented in Figure 6A (colored dots) with overlaid fits (colored continuous lines) for a two-compartment, uni-directional, first-order kinetic model as previously published (11). The values reported for the rates of the metabolic conversion of choline to phosphocholine using this type of compartmental model are: $r_{1A} = 0.0041\ s^{-1}$, $r_{1B} = 0.024\ s^{-1}$, $k_{AB} = 0.0015176\ s^{-1}$. The residuals of the choline and phosphocholine fits are shown in Figure 6C and display nonrandom structured residuals indicating that the chosen model is not adequate to fit the experimental data. In Figure 6E, the MEM/NLS shows the kinetic rates that characterize the fit curves of the experimental data obtained using a two-compartments, uni-directional compartmental model as previously published ($\lambda_{1A} = 0.0057\ s^{-1}$, $\lambda_{1B} = 0.0245\ s^{-1}$, $\lambda_{2B} = 0.0057\ s^{-1}$) (11). Figures 6B and F show the fits to the experimental data using the MEM/NLS algorithm and the kinetic rates derived, respectively. Two rates were identified for the time-signal curves of both choline ($\lambda_{1A} = 0.0104 s^{-1}$, $\lambda_{2A} = 0.0039 s^{-1}$, $n = 1$) and phosphocholine ($\lambda_{1B} = 0.0138 s^{-1}$, $\lambda_{2B} = 0.0086 s^{-1}$, $n = 1$). The SNR_B values calculated for this dataset was 25 (a.u.) in agreement with the values used in the Monte Carlo simulations.

DISCUSSION

Results from the analysis of simulated and experimental data suggest that the MEM/NLS method is adequate for the kinetic characterization of hyperpolarized dynamic time-series. The proposed analysis method is able to derive the number of kinetic rates from the time-series of compartment A and B for both compartmental models simulated. The estimation of the values of A_i and λ_i is affected by the presence of the noise in the data, nevertheless we showed that it is possible to derive the value of the characteristic kinetic rates (r_{1A}, r_{1B}, k_{AB} and k_{BA}) of the system studied by solving Eqs. [A3–A6] and Eqs. [A10–A14] (see Appendix) for bi- and uni-directional systems, respectively. The accuracy in estimating the value of k_{AB} with the MEM/NLS algorithm was comparable with that of conventional compartmental modeling

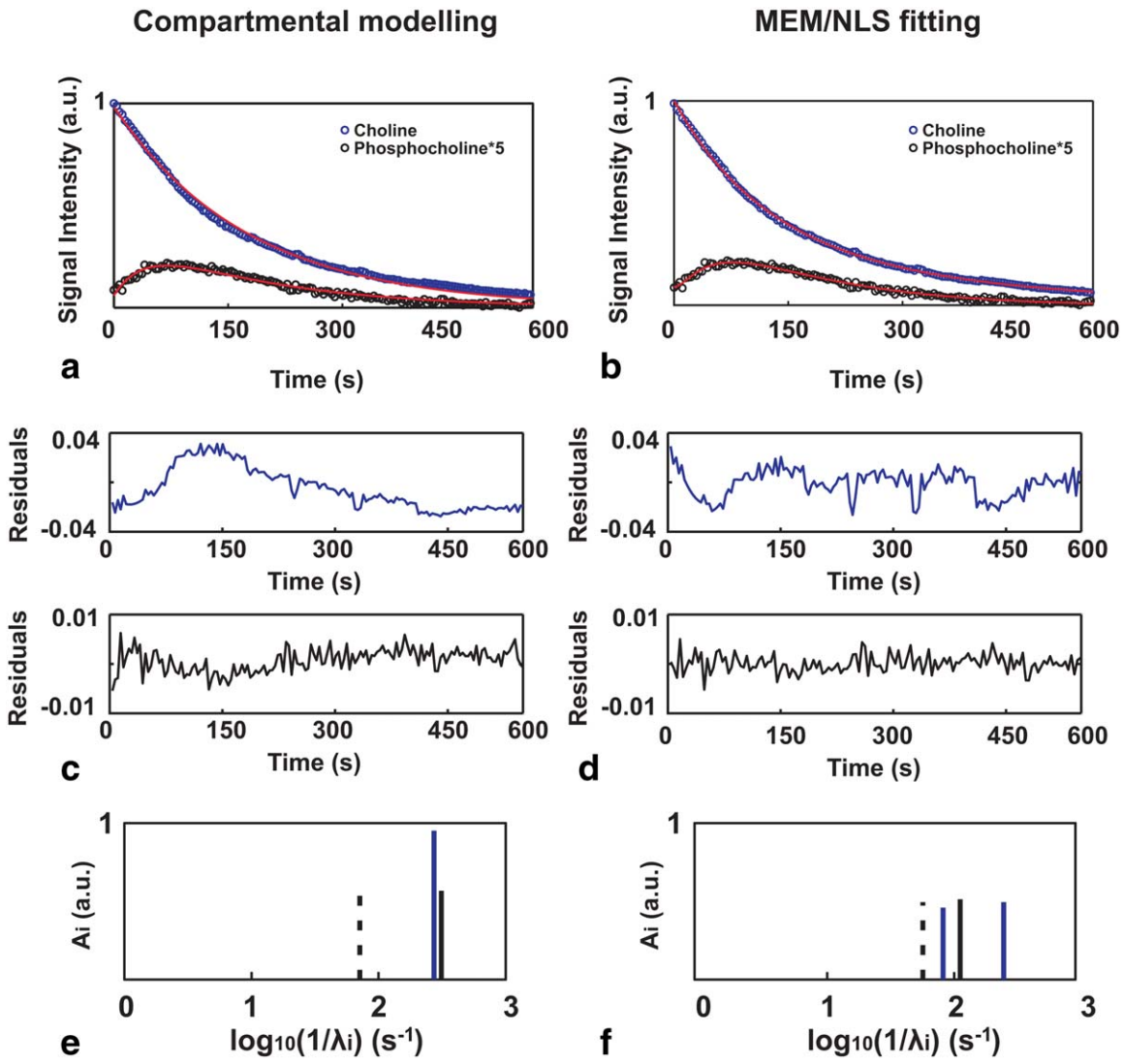

FIG. 6. **a:** ^{15}N time-series of choline (blue) and phosphocholine (black) with a fit obtained assuming one way first order reaction kinetics (continuous lines). **c:** Shows the nonrandom distribution of the residuals due to the inability of the chosen kinetic model to accurately describe the experimental data. **b**: Experimental data are plotted with overlaid fits from the hybrid MEM/NLS method for choline (blue) and phosphocholine (black), respectively. **d:** The random residuals resulted from this fitting are shown. The spectra of discrete rates suggested by a two-compartment, uni-directional kinetic model are shown (**e**), whereas those identified by the MEM/NLS fit are plotted (**f**). Solid and dashed lines correspond to rates with positive and negative amplitude, respectively.

for both types of systems, whereas the hybrid method overestimated the values of k_{BA} at low values of the rate constant.

MEM/NLS fits of the relaxation curves of hyperpolarized [1-^{13}C] pyruvate in solution acquired using three different flip angles (Fig. 4) identified only one kinetic rate, consistent with mono-exponential decays. The values of the relaxation rates of pyruvate derived with the proposed method are in excellent agreement with those derived by fitting with a mono-exponential function and with those previously published (18). From our data we calculated the influence of the flip-angle correction on the decay of the hyperpolarized signal and found the actual flip-angle to be less than the nominal flip-angle. Flip-angle calibration was carried out on a thermally polarized pyruvate sample. We do not pursue this further here although possible reasons for this include nonlinearity of the RF amplifiers at low flip-angle or the influence of radiation damping in highly polarized samples.

We applied the hybrid MEM/NLS algorithm to in vitro hyperpolarized ^{13}C time-series of pyruvate-lactate exchange in whole blood cells (Fig. 5). MEM/NLS identified a single rate from the pyruvate curve, whereas two rates were detected from the lactate time-series. The conversion of pyruvate to lactate catalyzed by LDH is an exchange reaction that is close to equilibrium. In the absence of other information, it would be therefore reasonable to fit the experimental data to a two-compartment, bi-directional kinetic model. MEM/NLS however identifies only a single rate for the pyruvate curve suggesting that the experimental data are better

described by a uni-directional model rather than a bi-directional system. Hyperpolarized pyruvate is transported across the cell membrane through specific monocarboxylate transporters. Once within the cytosol the intracellular pyruvate is in exchange with intracellular lactate through LDH. Extracellular pyruvate does not exchange directly with intracellular lactate. Modeling the metabolic conversion of pyruvate to lactate using a two-compartment, bi-directional kinetic model assumes that the hyperpolarized signal of pyruvate is from the intracellular rather than extracellular compartment. This is only true if the uptake of pyruvate across the cell membrane is faster than the rate of conversion of pyruvate to lactate. If the pyruvate uptake is slower than the rate of metabolic conversion then the hyperpolarized pyruvate signal will be dominated by the extracellular rather than intracellular compartment and transport may be rate limiting. In this case the system is better approximated by a two-compartment, uni-directional kinetic model where the compartment A represents the extracellular pyruvate, whereas compartment B represents the intracellular lactate. This information is lost if the experimental data are analyzed with a compartment model assuming a priori a bi-directional model. The values of k_{AB} for the conversion of pyruvate to lactate derived using Eqs. [A10–A13] were found to be in very good agreement with those estimated using conventional compartmental modeling and with those previously published (15).

The utility of the hybrid method for the analysis of hyperpolarized dynamic data was also considered by re-analyzing hyperpolarized ^{15}N choline data previously published. Fitting with MEM/NLS demonstrated less structured residuals and improved model fit performance (Figs. 6C and D). Of interest, with MEM/NLS two rates were suggested to describe the choline (compartment A) curve and two for the phosphocholine (compartment B) (Fig. 6F) in contrast with the use of a uni-directional kinetic model (Fig. 6E). These were $\lambda_{1A} = 0.0104\ s^{-1}$ and $\lambda_{2A} = 0.0039\ s^{-1}$, with the slowest corresponding to the $r_{1c} = 1/T_{1c}$ of choline. The two exponentials derived from the choline time-series could be compatible with a bi-directional enzymatic conversion. However, ^{31}P spectra acquired from the same solution before and after adding hyperpolarized choline demonstrated the presence of only ATP before the reaction and only ADP + PCho after the reaction, respectively (data not shown) (11). These experimental findings suggest that there was no back enzymatic conversion of phosphocholine to choline as expected for the enzyme choline kinase. We speculate that the appearance of an additional rate in the choline curve suggests that the reaction stopped during the time-course and this can be explained by second order kinetics of the enzymatic conversion. It has been previously shown that choline kinase activity is inhibited by ATP depletion and ADP accumulation as well as by product inhibition by phosphocholine (19). In this experiment a 20 mM hyperpolarized choline solution was added to purified human choline kinase containing 10 mM ATP and therefore the reaction was limited by the co-factor concentration, suggesting the importance of cofactor depletion during uni-directional reaction kinetics of hyperpolarized substrates.

We showed that the MEM/NLS algorithm is an adequate tool for the kinetic analysis of in vitro hyperpolarized dynamic data; however, our study has some limitations to be considered. We tested the sensitivity to noise of the hybrid method only for a range of SNR_Bs typical of in vitro experiments ($20 < SNR_B < 90$). Hyperpolarized time-series acquired in vivo exhibit higher noise levels than those detected in vitro. The performance of the MEM/NLS algorithm at lower SNR_Bs should, therefore, be accurately assessed before extending the method to the analysis of in vivo data. This was beyond the scope of this work, which is a proof of concept analysis of the applicability of the hybrid method to hyperpolarized data. Extending the method to the analysis of in vivo data also requires further consideration on the input function. The measurement of the optimal input function during hyperpolarized in vivo experiments is still an unsolved problem. The hyperpolarized signal of the injected molecule in the region of interest (ROI) cannot be used as an input function because it contains information on the delivery of the molecule but also on its metabolic conversion. Recent studies have proposed methods to obtain an accurate measure of the delivery input function directly by measuring the hyperpolarized signal of the injected molecule in the arterial blood or indirectly by detecting the hyperpolarized signal of urea, a non metabolically active compound, injected into the system at the same time of the metabolite of interest (20,21). With an accurate knowledge of the delivery input function, the hyperpolarized time-series of detected metabolites can be deconvoluted before applying the MEM/NLS algorithm. From a mathematical point of view, MEM/NLS represents only one of the different possibilities to solve the problem of fitting a set of unknown exponential decaying functions (Eq. [2]). The solutions proposed for positron-emitting radiolabeled compounds (22–25) offer an alternative for hyperpolarized data analysis but they need to be tested in the specific context.

CONCLUSIONS

This work is the proof of concept analysis of the feasibility of using the hybrid MEM/NLS method proposed by *Steinbach J.P. and colleagues* for the kinetic analysis of hyperpolarized in vitro data with minimum a priori assumption of the metabolic conversion studied. We demonstrated that this method is adequate to derive the number of kinetic rates that best describe the hyperpolarized ^{13}C MR time-series and how this can be used to inform on details of the enzymatic conversions that could otherwise be ignored if the experimental data were analyzed with traditional compartmental models where the type of reaction is assumed a priori. We also showed that it is possible to derive the value of the rates characteristic of the metabolic conversion by associating a compatible compartmental model to the MEM/NLS solution. However, results show that compartmental modeling is more accurate in estimating the values of the unknown kinetic parameters than MEM/NLS. The analysis approach presented here therefore will be useful to inform on the

compartmental model that best approximate the biological system observed using hyperpolarized ^{13}C MR especially when the metabolic pathway assessed is complex or a new hyperpolarized probe is used.

ACKNOWLEDGMENTS

The authors acknowledge financial support from the Department of Health by means of the National Institute for Health Research (NIHR) comprehensive Biomedical Research Centre award to Guy's & St Thomas' NHS Foundation Trust in partnership with King's College London and King's College Hospital NHS Foundation Trust. The work was also funded by an Engineering and Physical Sciences Research Council Ph.D. studentship and a British Heart Foundation project grant PG/10/20/28211 and award RE/08/003, and the Centre of Excellence in Medical Engineering Center funded by the Wellcome Trust and EPSRC under grant number WT088641/Z/09/Z, and the King's College London and UCL Comprehensive Cancer Imaging Center. The views expressed are those of the author and not necessarily those of the NHS, the NIHR or the Department of Health. TRE is grateful for support from the CRUK and EPSRC Cancer Imaging Center in association with the MRC and the Department of Health (England) grant C1060/A10334. The authors also would like to thank Dr. Matthew R. Orton for valuable advice and discussions.

APPENDIX

Assuming to have as input to the MEM/NLS algorithm two time-series representing the evolution in time of the MR signal of the hyperpolarized molecule A and its downstream metabolite B acquired in vitro (impulse input function) a general MEM/NLS solution can be written as in Eq. [2]. After deriving the unknown parameters n, A_i and λ_i for both metabolites it is possible to associate a compatible compartmental model.

For example, if $n = 2$ for both metabolites then a compatible model would be a two-compartment, bi-directional model shown in Figure 1. The solution of the Bloch-McConnell equations for this type of compartmental model is:

$$M_A(t) = \frac{A_0[(k_{AB} + r_{1A} - \lambda_2)e^{-t\lambda_1} + (k_{BA} + r_{1B} - \lambda_2)e^{-t\lambda_2}]}{\lambda_1 - \lambda_2} \quad [A1]$$

$$M_B(t) = \frac{A_0 k_{AB}(e^{-t\lambda_2} - e^{-t\lambda_1})}{\lambda_1 - \lambda_2} \quad [A2]$$

Under this hypothesis the amplitudes (A_i) and rates (λ_i) in Eq. [2] for a two-compartment, bi-directional kinetic model described by Eqs. [A1] and [A2] are:

$$A_{1A} = M_0(k_{AB} + r_{1A} - \lambda_2)/(\lambda_1 - \lambda_2) \quad [A3]$$

$$A_{2A} = M_0(k_{AB} + r_{1B} - \lambda_2)/\ (\lambda_1 - \lambda_2) \quad [A4]$$

$$A_{1B} = M_0 k_{AB}/(\lambda_1 - \lambda_2) \quad [A5]$$

$$A_{2B} = -M_0 k_{AB}/(\lambda_1 - \lambda_2) \quad [A6]$$

$$\lambda_{1,2} = \frac{-(r_{1A} + r_{1B} + k_{AB} + k_{BA}) \pm \sqrt{((r_{1B} + k_{BA}) - (r_{1A} + k_{AB}))^2 + 4k_{AB}k_{BA}}}{2} \quad [A7]$$

Where A_{iA} and A_{iB} represent the amplitudes of the rates derived for compartment A and B, respectively.

If $n = 1$ for compartment A and $n = 2$ for compartment B then a two-compartment, unidirectional model would be compatible.

The solution of the Bloch-McConnell equations for this type of compartmental model is:

$$M_A(t) = M_0 e^{-t\lambda_1} \quad [A8]$$

$$M_B(t) = \frac{M_0 k_{AB}(e^{-t\lambda_1} - e^{-t\lambda_2})}{k_{AB} + r_{1A} - r_{1B}} \quad [A9]$$

The relationship between the rates and the amplitudes derived with MEM/NLS and those characteristic of a two compartment, uni-directional reaction system is:

$$A_{1A} = M_0 \quad [A10]$$

$$A_{1B} = M_0 k_{AB}/(k_{AB} + r_{1A} - r_{1B}) \quad [A11]$$

$$A_{1B} = -M_0 k_{AB}/(k_{AB} + r_{1A} - r_{1B}) \quad [A12]$$

$$\lambda_1 = k_{AB} + r_{1A} \quad [A13]$$

$$\lambda_2 = r_{1B} \quad [A14]$$

By solving the system of linear algebraic equations (Eqs. [A3–A6] or [A10–A14]), it is possible to derive the unknown parameters M_0, r_{1A}, r_{1B}, k_{AB}, and k_{BA}.

REFERENCES

1. Day SE, Kettunen MI, Gallagher FA, Hu DE, Lerche M, Wolber J, Golman K, Ardenkjaer-Larsen JH, Brindle KM. Detecting tumor response to treatment using hyperpolarized 13C magnetic resonance imaging and spectroscopy. Nat Med 2007;13:1382–1387.
2. Schroeder MA, Cochlin LE, Heather LC, Clarke K, Radda GK, Tyler DJ, Shulman RG. In vivo assessment of pyruvate dehydrogenase flux in the heart using hyperpolarized carbon-13 magnetic resonance. Proc Natl Acad Sci U S A 2008;105:12051–12056.
3. Hu S, Chen AP, Zierhut ML, Bok R, Yen YF, Schroeder MA, Hurd RE, Nelson SJ, Kurhanewicz J, Vigneron DB. In vivo carbon-13 dynamic MRS and MRSI of normal and fasted rat liver with hyperpolarized 13C-pyruvate. Mol Imaging Biol 2009;11:399–407.
4. Park JM, Recht LD, Josan S, Merchant M, Jang T, Yen YF, Hurd RE, Spielman DM, Mayer D. Metabolic response of glioma to dichloroacetate measured in vivo by hyperpolarized (13)C magnetic resonance spectroscopic imaging. Neuro Oncol 2013;15:433–441.
5. Harris T, Eliyahu G, Frydman L, Degani H. Kinetics of hyperpolarized 13C1-pyruvate transport and metabolism in living human breast cancer cells. Proc Natl Acad Sci U S A 2009;106:18131–18136.
6. Menichetti L, Frijia F, Flori A, et al. Assessment of real-time myocardial uptake and enzymatic conversion of hyperpolarized [1–13C] pyruvate in pigs using slice selective magnetic resonance spectroscopy. Contrast Media Mol Imaging 2012;7:85–94.
7. Cunningham VJ, Jones T. Spectral analysis of dynamic PET studies. J Cereb Blood Flow Metab 1993;13:15–23.
8. Bertoldo A, Vicini P, Sambuceti G, Lammertsma AA, Parodi O, Cobelli C. Evaluation of compartmental and spectral analysis models of [18F]FDG kinetics for heart and brain studies with PET. IEEE Trans Biomed Eng 1998;45:1429–1448.

9. Steinbach PJ, Ionescu R, Matthews CR. Analysis of kinetics using a hybrid maximum-entropy/nonlinear-least-squares method: application to protein folding. Biophys J 2002;82:2244–2255.
10. Cobelli C, Foster D, Toffolo G. Tracer kinetics in biomedical research. New York: Springer; 2000.
11. Gabellieri C, Reynolds S, Lavie A, Payne GS, Leach MO, Eykyn TR. Therapeutic target metabolism observed using hyperpolarized 15N choline. J Am Chem Soc 2008;130:4598–4599.
12. Istratov AA, Vyvenko OF. Exponential analysis in physical phenomena. Rev Sci Instrum 1999;70:1233–1257.
13. Mohammad-Djafari A, Giovannelli JF, Demoment G, Idier J. Regularization, maximum entropy and probabilistic methods in mass spectrometry data processing problems. Int J Mass Spect 2002;215:175–193.
14. Hill DK, Orton MR, Mariotti E, et al. Model free approach to kinetic analysis of real-time hyperpolarized 13C magnetic resonance spectroscopy data. PLoS One 2013;8:e71996.
15. Hill DK, Jamin Y, Orton MR, Tardif N, Parkes HG, Robinson SP, Leach MO, Chung YL, Eykyn TR. (1)H NMR and hyperpolarized (1)(3)C NMR assays of pyruvate-lactate: a comparative study. NMR Biomed 2013;26:1321–1325.
16. Santarelli MF, Positano V, Giovannetti G, et al. How the signal-to-noise ratio influences hyperpolarized 13C dynamic MRS data fitting and parameter estimation. NMR Biomed 2012;25:925–934.
17. Weiss K, Mariotti E, Hill DK, Orton MR, Dunn JT, Medina RA, Southworth R, Kozerke S, Eykyn TR. Developing hyperpolarized C-13 spectroscopy and imaging for metabolic studies in the isolated perfused rat heart. Appl Magn Reson 2012;43:275–288.
18. Wilson DM, Keshari KR, Larson PE, et al. Multi-compound polarization by DNP allows simultaneous assessment of multiple enzymatic activities in vivo. J Magn Reson 2010;205:141–147.
19. Kim KH, Voelker DR, Flocco MT, Carman GM. Expression, purification, and characterization of choline kinase, product of the CKI gene from Saccharomyces cerevisiae. J Biol Chem 1998;273:6844–6852.
20. Kazan SM, Reynolds S, Kennerley A, Wholey E, Bluff JE, Berwick J, Cunningham VJ, Paley MN, Tozer GM. Kinetic modeling of hyperpolarized C-13 pyruvate metabolism in tumors using a measured arterial input function. Magn Reson Med 2013;70:943–953.
21. von Morze C, Larson PEZ, Hu S, Yoshihara HAI, Bok RA, Goga A, Ardenkjaer-Larsen JH, Vigneron DB. Investigating tumor perfusion and metabolism using multiple hyperpolarized C-13 compounds: HP001, pyruvate and urea. Magn Reson Imaging 2012;20:305–311.
22. Gunn RN, Gunn SR, Turkheimer FE, Aston JA, Cunningham VJ. Positron emission tomography compartmental models: a basis pursuit strategy for kinetic modeling. J Cereb Blood Flow Metab 2002;22:1425–1439.
23. Turkheimer FE, Hinz R, Gunn RN, Aston JA, Gunn SR, Cunningham VJ. Rank-shaping regularization of exponential spectral analysis for application to functional parametric mapping. Phys Med Biol 2003; 48:3819–3841.
24. Veronese M, Bertoldo A, Bishu S, Unterman A, Tomasi G, Smith CB, Schmidt KC. A spectral analysis approach for determination of regional rates of cerebral protein synthesis with the L-[1-(11)C]leucine PET method. J Cereb Blood Flow Metab 2010;30:1460–1476.
25. Mariotti E, Veronese M, Dunn JT, Medina RA, Blower PJ, Southworth R, Eykyn TR. Assessing radiotracer kinetics in the Langendorff perfused heart. EJNMMI Res 2013;3:74.